

---

## MODELLING THE ARCTIC STABLE BOUNDARY LAYER AND ITS COUPLING TO THE SURFACE

G. J. STEENEVELD\*, B. J. H. VAN DE WIEL and A. A. M. HOLTSLAG  
*Wageningen University, Meteorology and Air Quality, Duivendaal 2, 6701 AP Wageningen,  
The Netherlands*

(Received in final form 12 May 2005)

**Abstract.** The impact of coupling the atmosphere to the surface energy balance is examined for the stable boundary layer, as an extension of the first GABLS (GEWEX Atmospheric Boundary-Layer Study) one-dimensional model intercomparison. This coupling is of major importance for the stable boundary-layer structure and its development because coupling enables a realistic physical description of the interdependence of the surface temperature and the surface sensible heat flux. In the present case, the incorporation of a surface energy budget results in stronger cooling (surface decoupling), and a more stable and less deep boundary layer. The proper representation of this is a problematic feature in large-scale numerical weather prediction and climate models. To account for the upward heat flux from the ice surface beneath, we solve the diffusion equation for heat in the underlying ice as a first alternative. In that case, we find a clear impact of the vertical resolution in the underlying ice on boundary-layer development: coarse vertical resolution in the ice results in stronger surface cooling than for fine resolution. Therefore, because of this impact on stable boundary-layer development, the discretization in the underlying medium needs special attention in numerical modelling studies of the nighttime boundary layer. As a second alternative, a bulk conductance layer with stagnant air near the surface is added. The stable boundary-layer development appears to depend heavily on the bulk conductance of the stagnant air layer. This result re-emphasizes the fact that the interaction with the surface needs special attention in stable boundary-layer studies. Furthermore, we perform sensitivity studies to atmospheric resolution, the length-scale formulation and the impact of radiation divergence on stable boundary-layer structure for weak windy conditions.

**Keywords:** Decoupling, GABLS, Radiation divergence, Resolution, Stable boundary layer, Surface energy balance.

### 1. Introduction

In the first GABLS (GEWEX Atmospheric Boundary-Layer Study) model intercomparison study (Holtslag et al., 2003) a large variation of the outputs of single column models is found (Cuxart et al., 2006). As such, a simple stable boundary layer is studied with a prescribed constant cooling rate

\* E-mail: Gert-Jan.Steeneveld@wur.nl

of  $-0.25 \text{ K h}^{-1}$  at the surface; such a forcing method for the stable boundary layer (SBL) is quite common (see e.g. Delage, 1974, 1997; Nieuwstadt and Driedonks, 1979; Kosovic and Curry, 2000).

Alternatively, the surface turbulent heat flux  $\overline{w'\theta'_s}$  can be prescribed (Galmarini et al., 1998; Viterbo et al., 1999). Although both methods are classical in the sense that they are easy to apply (especially in theoretical studies), there seems no direct physical justification for either one. In fact, the presence of feedbacks between the surface temperature ( $T_s$ ), the surface sensible heat flux and the heat flux from the underlying medium towards the surface is essential (Derbyshire, 1999). Changes in surface-layer stability will affect the sensible heat flux through the stability functions, and consequently, the surface temperature will be affected through a coupled surface energy budget.

In the case of a surface energy budget, we can raise the question as to how the turbulent sensible heat flux in the SBL will react to surface cooling (Derbyshire, 1999; Delage et al., 2002). In fact the sensible heat flux may react in two different ways, corresponding to two regimes (compare also De Bruin, 1994; Derbyshire, 1999):

- The first is the weakly stable case, in which the sensible heat flux increases with stability. A sudden increase in stratification leads to a larger heat flux, opposing the increased stratification (negative feedback).
- The second is the very stable case, in which an increase in stratification leads to a reduction of the sensible heat flux and therefore intensifying the increased stratification (positive feedback). This may lead to a collapse of turbulence so that the actual SBL decouples from the surface (ReVelle, 1993; Coulter and Doran, 2002; Delage et al., 2002; van de Wiel et al., 2004).

Note that, besides the above subdivision, alternative SBL classifications have been proposed by Beyrich (1997), Mahrt et al. (1998), van de Wiel et al. (2003) and Mahrt and Vickers (2002) and others. At present no general classification picture of the SBL exists. Therefore, in the current work we use the pragmatic subdivision indicated above, i.e: weakly stable and very stable conditions.

From observations it is known that the SBL may either remain in a decoupled state, or recouple after a certain time, leading to turbulence of an intermittent character (van de Wiel et al., 2002a). From a modelling perspective, this very stable regime often leads to practical problems: for example large-scale atmospheric models tend to decouple and remain decoupled in an *unphysical sense* (e.g. Louis, 1979; Derbyshire, 1999). This can result in a serious cold model bias, especially during conditions where

strong stratification exists for longer periods such as in the polar region in wintertime (Viterbo et al., 1999). To circumvent this problem, large-scale atmospheric models apply artificial enhanced mixing formulations for turbulence in the case of strong stability (e.g. Louis, 1979; Beljaars and Holtslag, 1991).

The importance of the surface-energy balance feedback was indicated by theoretical considerations above. The relevance of this feedback can also directly be inferred from typical observations of the surface temperature. van de Wiel et al. (2003) illustrate, using observations from the CASES-99 experiment, that the surface temperature  $T_s$ , the turbulent heat flux and the soil heat flux may show simultaneous rapid changes during the night, revealing their interdependence. These fluctuations (with a rather high frequency compared to the daily cycle) are important for the dynamics of the SBL as a whole and cannot be modelled without taking into account the mutual interactions between the surface temperature, the sensible heat flux and the underlying soil. Derbyshire (1999) concludes: "Even the simplest valid analysis needs to couple the wind profile, the temperature profile and the surface heat budget".

Steenefeld et al. (2004) reveal that one-dimensional modelling results are largely improved as compared to detailed in situ observations when:

- (a) an accurate vegetation layer and fine soil discretisation are applied, and
- (b) radiation divergence is included, at least for low geostrophic winds.

Figure 1 shows results of the modelled vegetation temperature (full line) for three consecutive diurnal cycles during the CASES-99 experiment (Steenefeld et al., 2004). The first night is intermittent turbulent (moderate stable), the second continuously turbulent (weakly stable) and the third night is 'non-turbulent' (very stable), with suppressed turbulence. Thus we cover a wide range of stability conditions in this experiment. A clear agreement is found between the model results and the observations for these three different types of nights. This result is remarkable given the fact that the surface temperature is a difficult quantity to predict accurately with an offline model, especially for such a broad range of stability classes (Best, 1998). Additionally, we find that (not shown) the modelled potential temperature ( $\theta$ ) profiles also compare well with boundary-layer observations for these particular case studies.

The dash-dotted line in Figure 1 shows the modelled surface temperature when the enhanced mixing approach is applied in the single column model, as is common practice in operational numerical weather prediction (NWP) and climate prediction models (e.g. Beljaars and Viterbo, 1998). Then the surface temperature is overestimated by about 5 K for the first two nights and the first half of the third night. Thus, even from a practical point of view (as in NWP), the enhanced mixing approach is not

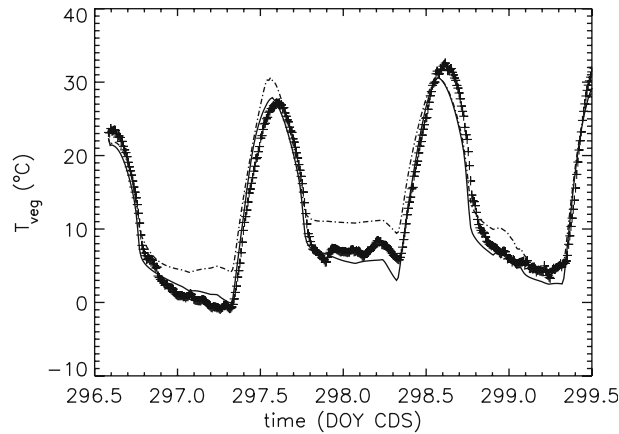


Figure 1. Modelled (full line) and observed (+) vegetation temperature for the period 23–26 October 1999 (Day of Year (DOY) = 296.5–299.5) for the CASES-99 experiment. The dash-dotted line indicates the model performance when enhanced mixing is applied.

appropriate over a large stability range. Figure 1 shows that an accurate prediction of *in situ* observations is possible using a sound physical representation of soil/vegetation, heat exchange processes, without the need for an (artificial) enhanced mixing formulation. Note that, in our current comparison with local observations, we disregard possible enhanced mixing as a consequence of spatial averaging issues such as addressed by Mahrt (1987), which may play an important role in NWP for the SBL under heterogeneous conditions.

The foregoing motivates us to pose the research question: what is the impact on the GABLS case study when we include realistic features of a surface energy balance? Therefore, we compare the outcome of the *reference case* (i.e. with prescribed surface cooling) with the results of *two alternative surface coupled cases*. Both alternatives explicitly solve the surface energy budget equation and apply

- the heat diffusion equation in the underlying ice (Alternative I), or
- use a bulk-conductance law at the surface (Alternative II),

in our extension of the single column model by Duynkerke (1991, 1999) to account for the heat flux from the underlying medium. This model also participated in the GABLS *reference case* comparison of various single column models (Cuxart et al., 2006).

Section 2 gives a short overview of the model description and additional results for the reference case study. Section 3 presents the results for a coupled system with a heat diffusion scheme (Alternative I). Results for Alternative II are presented in Section 4. Conclusions and recommendations are given in Section 5.

## 2. Reference Case: Model Description and Results

### 2.1. MODEL DESCRIPTION

Our model is an extension of the model described by Duynkerke (1991, 1999). Turbulent mixing is parameterised in terms of local gradients (assuming local equilibrium of the turbulent kinetic energy (TKE) budget):

$$\overline{w'\chi'} = -K_x \frac{\partial X}{\partial z}, \quad (1)$$

where  $X$  is a mean quantity,  $\overline{w'\chi'}$  the turbulent flux of  $X$ , and  $z$  the height above the surface. The eddy diffusivity ( $K$ ) is given by first-order closure, expressed as (see also Holtslag, 1998):

$$K_x = \frac{l^2}{\phi_m \phi_x} \left| \frac{\partial \vec{V}}{\partial z} \right| \quad x \in \{m, h\}, \quad (2)$$

with the mixing length  $l = kz$  and  $x = m$  for momentum and  $x = h$  for heat,  $k$  the Von Kármán constant and  $\partial \vec{V} / \partial z$  the vector wind shear. Based on reanalysis of the Cabauw tower observations from Nieuwstadt (1984), Duynkerke (1991) proposed the stability function

$$\phi_x(\zeta) = 1 + \beta_x \zeta \left( 1 + \frac{\beta_x}{\alpha_x} \zeta \right)^{\alpha_x - 1}, \quad (3)$$

where  $\zeta = z/\Lambda$ ,  $\Lambda$  is the local Obukhov length, defined as  $\Lambda = -\bar{\theta} u_{*L}^3 / (kg \overline{w'\theta'})$ , and  $u_{*L}$  is the local friction velocity. Coefficients were found to be  $\beta_m = 5$ ,  $\alpha_m = 0.8$ ,  $\beta_h = 7.5$  and  $\alpha_h = 0.8$ , as compared to the original findings of Nieuwstadt (1984) who found  $\alpha_h = \alpha_m = 1$ , and  $\beta_m = \beta_h = 5$ . Note that the coefficients used in the present study (viz. as in Duynkerke, 1991) are in close agreement with the prescribed coefficients for the surface layer in the intercomparison case, especially for the weakly stable part.

Thus a simple first-order closure model for turbulence is used in the present model, because the main aim is to illustrate the impact of coupling the atmosphere to the surface. Moreover, as shown by Brost and Wyngaard (1978), TKE transport terms in the SBL are usually relatively small so that the local equilibrium assumption is often applicable. Radiation divergence is neglected in the reference case.

The GABLS reference case study is defined over an ice surface with a relatively large roughness length for momentum and heat of  $z_0 = z_{0h} = 0.1$  m; the geostrophic wind is  $u_g = 8$  m s<sup>-1</sup>,  $v_g = 0$  m s<sup>-1</sup> and the Coriolis parameter  $f = 1.39 \times 10^{-4}$  s<sup>-1</sup> (equivalent to 73° N). The initial mean state is given by  $\theta = 265$  K for  $0 < z < 100$  m and 0.01 K m<sup>-1</sup> increasing above  $z > 100$  m, and the atmosphere is considered to be dry. The model integration is for 9 h, and

TABLE I

Overview of integrated cooling in the SBL for the different methods.

Case study	Integrated cooling (K m)
Reference study	-342
Equation 5	-242
Diffusion scheme	-611
Bulk conductance ( $\lambda_m/\delta_m=5$ )	-736

for the current study we apply a 40-layer logarithmically spaced grid, providing fine resolution near the surface ( $\Delta z = 0.7$  m) and coarser near the top of the domain (800 m in total). For additional information we refer to Beare et al. (2006) and Cuxart et al. (2006).

## 2.2. RESULTS REFERENCE CASE

Figure 2 shows the evolution of the potential temperature (a) and wind speed (b) profile for the GABLS intercomparison study with prescribed surface temperature, shown as a *reference*. For convenience we use the integrated cooling (*IC*) of the boundary layer as a useful measure to compare several model runs. *IC* is defined as:

$$IC = \int_{z=0}^{z=z_{TOP}} \{\theta_{start}(z) - \theta_{final}(z)\} dz \quad (4)$$

in which  $z_{TOP}$  is the top of the model domain. For the reference case study *IC* amounts to  $-342$  K m after 9 h (Table I).

The reference case uses the classical length scale  $l = kz$ , which is valid near the surface. Besides this length scale, several additional turbulent length scale ( $l$ ) formulations are currently in use (Cuxart et al., 2006), the rationale being that  $z$  is not the only governing length scale when the stratification becomes strong. One of the simplest extensions to this neutral length scale ( $l = kz$ ) is (Nieuwstadt, 1984; Hunt et al., 1985):

$$\frac{1}{l} = \frac{1}{kz} + \frac{N}{\sigma_w}, \quad (5)$$

in which  $N$  is the Brunt-Vaisälä frequency, and we *a priori* parameterize the standard deviation of vertical velocity  $\sigma_w$  by  $\sigma_w = 1.3u_{*L}$  (Nieuwstadt, 1984).

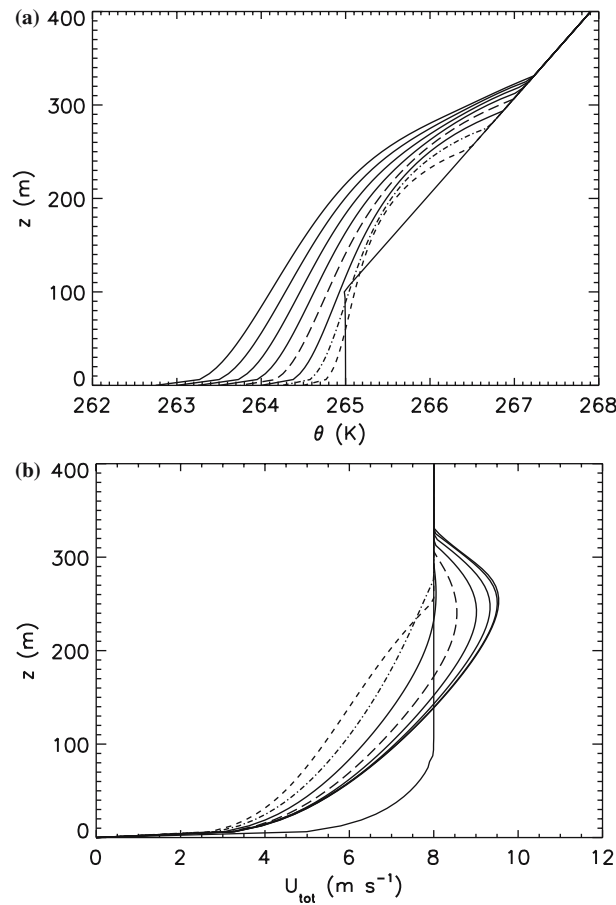


Figure 2. Potential temperature (a) development and structure for the reference GABLS case study with prescribed surface temperature, (b) for wind speed (vector sum). Profiles are drawn every hour, (dashes: after 1 h; dash dot after 2 h; dash dot-dot-dot after 3 h; long dashes after 4 h; after 5 h: full lines).

Figure 3 gives the comparison of the final profiles for potential temperature (a) and wind speed (b) in comparison with the large-eddy simulation (LES) results for the GABLS case study (ensemble mean) and the LES of Wageningen University. Naturally, the strongest impact of mixing length formulation is found at the top where the inversion is strongest.

The results of Equation (5) are in surprisingly good agreement with those from the LES models. This is in contrast to the original length scale formulation in which  $l = kz$ , which produces too much vertical mixing. Note that, in principle, it is expected that modification of Equation (3) for high stabilities would be equivalent to our mixing length modifications. Using Equation (5),  $IC$  amounts to  $-242 \text{ K m}$  (Table I). For the remainder

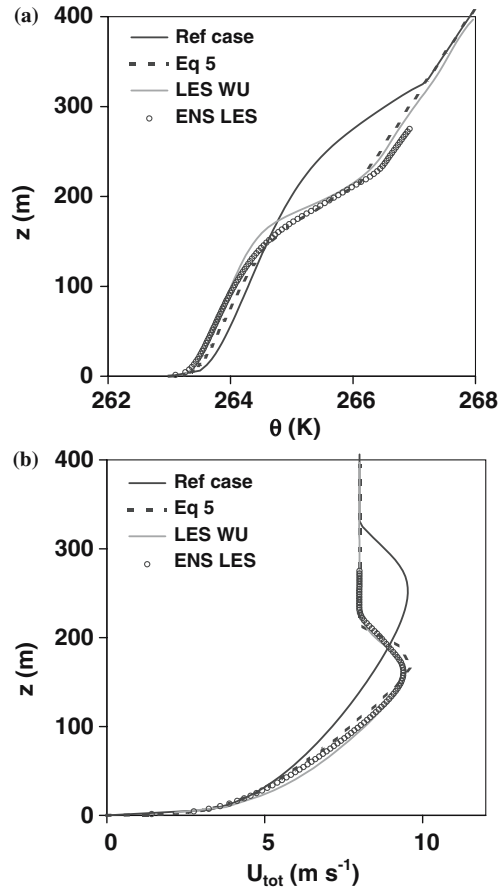


Figure 3. Final profiles of potential temperature (a) and wind speed (b) for the reference case, LES and Equation (5).

of this paper we retain the original formulation, Equation (3), as this was also used in the GABLS model intercomparison study.

The impact of vertical resolution for the *reference* case was examined by performing model simulations at a 6.25-m and a 40-m linear grid mesh (typical resolution for operational model) and a 40-layer stretched grid with fine grid mesh near the surface. No significant differences between these model runs were found (not shown), which agrees with the results of Delage et al. (1997) and Cuxart et al. (2006). However, care must be taken when interpreting these results, since this invariance may be caused by the prescribed surface temperature, which fixes partly the structure of the SBL.

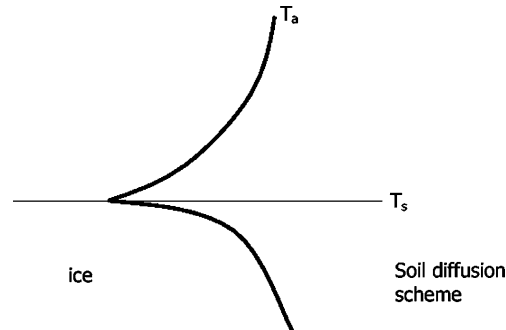


Figure 4. Model set-up for the SBL coupled with the ice through a heat diffusion scheme.

### 3. Coupling to the Surface with a Heat Diffusion Scheme (Alternative I)

#### 3.1. GENERAL

The reference case study (see before in Section 2 and in Cuxart et al., 2006) uses a prescribed surface-cooling rate of  $-0.25 \text{ K h}^{-1}$ . As mentioned before, this method gives only a limited degree of freedom, and therefore may limit our understanding of real SBL dynamics. Therefore, the current study goes one step further and focuses on the interdependence of the surface temperature ( $T_s$ ) and the surface sensible heat flux  $\overline{w'\theta'_s}$ , by introducing the surface energy budget. The net radiation as computed by the radiation scheme is an essential element in the coupling to the boundary-layer scheme. The longwave radiation components (upward and downward) are calculated using the grey-body approximation of Garratt and Brost (1981, from now on referred to as GB81). As a first test the current model set-up has been evaluated using the cases of Estournel and Guedalia (1985), and the results were found to be similar. For the present study we use a surface emissivity  $\varepsilon_s = 0.96$  for ice (Oke, 1978), together with a uniform specific humidity profile of  $q = 1 \times 10^{-4} \text{ kg kg}^{-1}$ . To consider the heat flux from the underlying medium towards the surface, we solve the diffusion equation for heat in a massive block of ice beneath the atmosphere (Figure 4a). Both the air temperature and surface temperature are free variables in this configuration and  $\overline{w'\theta'_s}$  and  $T_s$  are related interdependently, as in reality. The ice has a vertical dimension of 0.75 m (sufficient for short time integrations) and is initialised as  $\theta_{\text{ice}} = 265 \text{ K}$ , with  $\theta_{\text{ice}}$  being held constant at the lower boundary during the simulation. In this manner, the ice supplies heat from below to the surface as a reaction to the surface cooling. The material properties used in the current study (using ice, see next section) are summarized in Table II.

TABLE II  
Material properties of ice (Oke, 1978).

Property	ICE
Density $\rho$ (kg m <sup>-3</sup> )	920
Diffusivity $K_s$ (m <sup>2</sup> s <sup>-1</sup> )	$1.16 \times 10^{-6}$
Heat capacity $C_{ice}$ (J kg <sup>-1</sup> K <sup>-1</sup> )	2100
Conductivity $\lambda_g$ (W m <sup>-1</sup> K <sup>-1</sup> )	2.24

The results of this simple atmosphere-surface coupling (Figure 4a) on the development of the SBL are shown in Figure 5. Compared to the reference case, this extension with a simple surface scheme results in a rather different SBL structure. Especially in the first hours, the surface cooling is much stronger than in the reference case (Figure 2). We observe that the boundary layer is less deep (220 m after 9 h) and experiences a stronger total surface cooling than in the reference case ( $\theta_{final} = 259.3$  K instead of 262.75 K after 9 h). The vertical structure of the SBL is modified: the low-level jet (LLJ) maximum is slightly weaker, at a lower level (160 m altitude) and sharper. The coupling with the surface for the present set-up causes a doubling of the extracted energy compared to the reference case, since  $IC$  equals  $-611$  K m.

### 3.2. IMPACT OF RESOLUTION

For the reference study without coupling, no serious dependence on vertical resolution in the atmosphere was found (see previous section). Interestingly, we will see that this is not true for the heat diffusion scheme in the ice. To examine the impact of resolution in further detail, we perform a sensitivity study on vertical resolution in the atmosphere and in the ice. As such, five model simulations are made with different kinds of vertical resolution (that apply both to the radiation scheme and the turbulence scheme, Table III):

- Both atmosphere (with a stretched grid typically  $\Delta z = 0.5$  m) and ice ( $\Delta z_{ice} = 0.005$  m) have fine resolution. This provides the reference run for the coupled case.
- Atmosphere has operational ( $\Delta z = 40$  m) and ice has fine ( $\Delta z_{ice} = 0.005$  m) resolution.
- Atmosphere has operational ( $\Delta z = 40$  m) and ice has coarse (five layers with  $\Delta z_{ice} = 0.25$  m) resolution. State-of-the-art numerical weather prediction and climate models adopt this typical configuration.

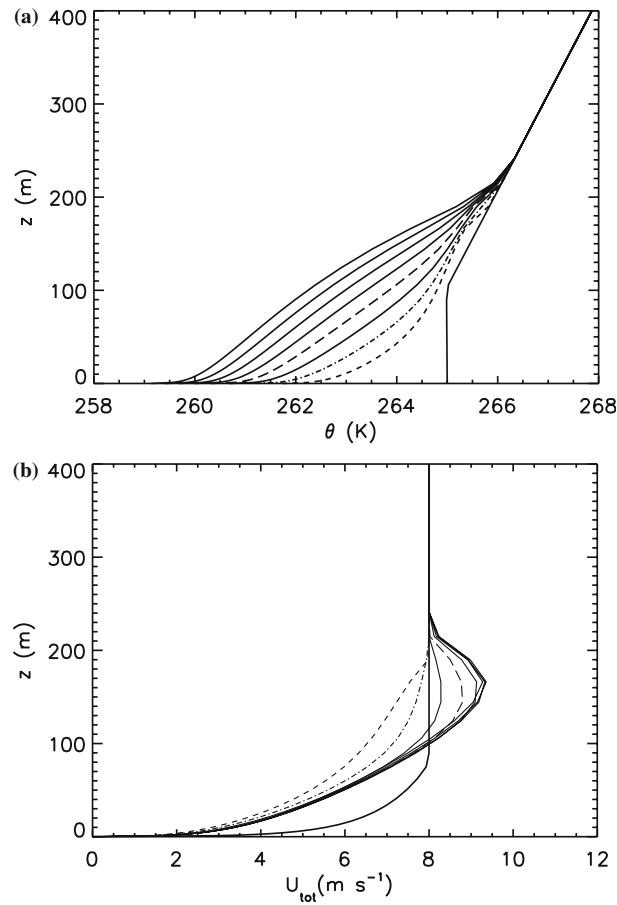


Figure 5. Potential temperature (a) and wind speed (b) development and structure for the alternative of solving the surface energy balance with a diffusion scheme for the ice heat flux.

TABLE III

Resolution in atmosphere and ice for different model sensitivity experiments

Run	Near-surface atmospheric resolution (m)*	Soil resolution (m)	Remark
I	0.5	0.005	Reference for coupled case
II	40	0.005	
III	40	0.25	Typical for NWP
IV	0.5	0.25	
V	40	0.25	Enhanced Turbulence

\* Using a 40-layer stretched grid.

- Atmosphere has fine resolution near the surface (with a stretched grid typically  $\Delta z = 0.5$  m) and the ice has coarse ( $\Delta z_{\text{ice}} = 0.25$  m) resolution.
- Atmosphere has operational resolution ( $\Delta z = 40$  m) applying *enhanced turbulent mixing* and the ice has coarse resolution ( $\Delta z_{\text{ice}} = 0.25$  m).

Figure 6 shows the final potential temperature (a) and wind speed profiles (b) for these five permutations. When we compare the final profile of the fine resolution and the operational resolution in the atmosphere, only a small difference is found *so long as fine resolution in the ice is used in both cases*. This supports the results of Delage (1997) who explains that the altitude of the first grid point is less important for calculating the turbulent fluxes at the surface, due to compensating effects. By choosing the first model level at higher altitude, the gradients of temperature and wind speed are smaller, which causes an underestimation of the flux. This is compensated for by a larger mixing length (since it is proportional to  $z$ ) and a slower increase of the bulk Richardson number with height. Both effects increase the estimated surface flux and more or less counteract the first effect.

With the ice having a coarser grid (both for the atmosphere at fine and operational grid mesh), the surface cooling is considerably larger and the SBL is less deep compared with the case with fine resolution in the ice. Two counteracting effects are present:

- thick ice slabs will cause the ice to cool more slowly because of its large heat capacity, and therefore slow down the surface cooling;
- the temperature gradients in the ice are smaller due to the larger grid length and consequently only a small heat flux to the surface can be maintained, resulting in a smaller heat flux from the ice. Overall, this gradient effect of a coarse resolution seems to dominate the heat capacity effect, leading to stronger surface cooling.

Apparently, the model results appear to be most sensitive to vertical resolution in the underlying medium when the model is in coupled mode. For completeness we mention that for the extreme case, when we compare the total system at fine resolution with the total system at coarse resolution, we find a surface temperature difference of about 2 K for this case study.

We can hypothesize whether the stronger surface cooling in the case of coarse resolution in the ice may be compensated in practice, e.g. by (artificial) enhanced turbulent mixing in the atmosphere (as in Louis, 1979). This is explored in Figure 6: when turbulent mixing is enhanced (by setting  $\alpha_m = \alpha_h = 0.85$  and  $\beta_m = \beta_h = 2.5$ ), together with a coarse resolution both in the atmosphere and the ice, the surface cooling is reduced partly and the boundary layer has thickened 30 m compared to the case without the enhanced mixing. However, from this figure it seems that lack of

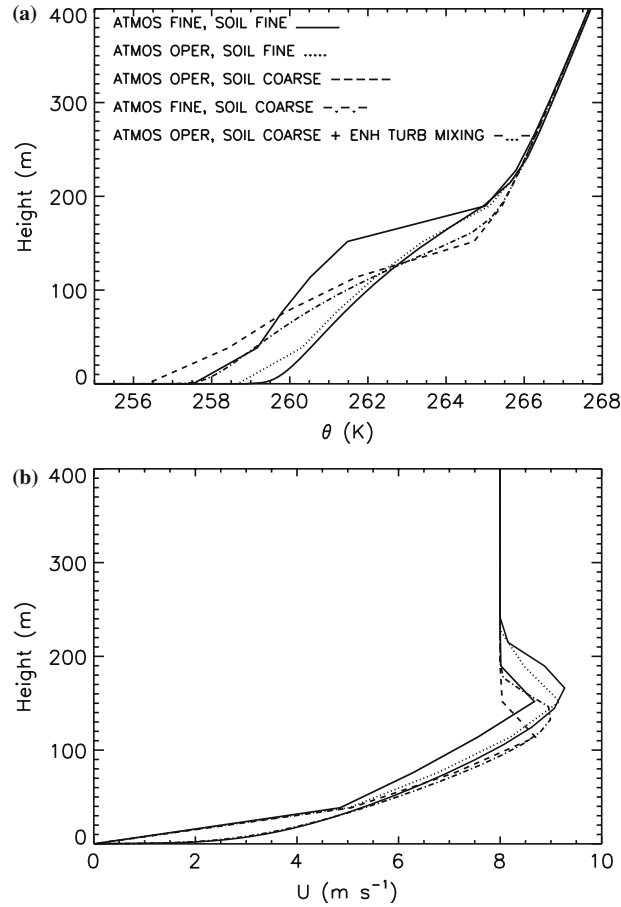


Figure 6. Final potential temperature (a) and wind speed (b) profiles as a function of vertical resolution in the atmosphere and the underlying ice.

resolution in the ice *cannot* be cancelled out by enhanced turbulent mixing in the atmosphere.

The excess atmospheric cooling in the case of grid coarsening in the underlying medium can be attributed to either turbulent cooling (divergence of sensible heat flux) or cooling by the radiation scheme. In this study, the enhanced cooling due to the grid coarsening in the ice is mainly caused by the turbulence scheme (increased flux divergence, not shown) and could not be attributed to the radiation scheme.

#### 4. Coupling to the Surface with a Bulk Conductance Layer (Alternative II)

A second approach to incorporating the surface energy budget (this is widely applied in numerical models: see, for example, Holtslag and

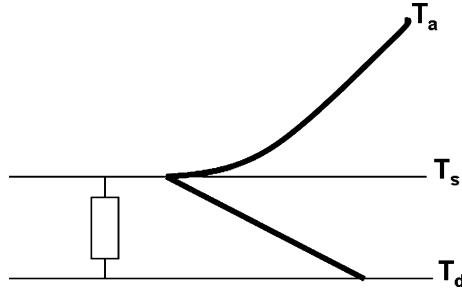


Figure 7. Model set-up for the SBL coupled with the ice through a bulk conductance layer of stagnant air (b).

De Bruin (1988); Duynkerke (1991); Viterbo and Beljaars (1995), is to incorporate a small isolating layer of stagnant air (see Figure 7) with a small heat capacity (Viterbo et al., 1999). For the current study, we will use a conductance layer to mimic the isolating properties of the stagnant layer. However, note that our intention is not to model the total mass and energy budgets of a snow layer; for that purpose, we refer to Koivusalo et al. (2001). In the current approach both the surface temperature and the air temperature are free variables and similar reasoning as in Section 3 is valid for  $\overline{w'\theta'_s}$ . This additional layer enables the surface temperature to react rapidly to imposed sudden changes in the surface cooling. The prognostic equation for the surface temperature in this case holds

$$C_v \frac{\partial T_s}{\partial t} = Q^* - \rho C_p \overline{w'\theta'_s} - \frac{\lambda_m}{\delta_m} (T_s - T_d), \quad (6)$$

where  $Q^*$  is the difference between the net radiation and latent heat flux, and in which  $C_v$  ( $\text{J m}^{-2} \text{K}^{-1}$ ) is the heat capacity of the stagnant air layer,  $\lambda_m/\delta_m$  ( $\text{W m}^{-2} \text{K}^{-1}$ ) is the bulk heat conductance for that layer and  $T_d$  (K) the deep ice temperature (Figure 7).

In this study we took  $T_d$  constant for simplicity; however, for long time scales a prognostic equation for  $T_d$  is required. The air density is given by  $\rho$  ( $\text{kg m}^{-3}$ ) and the air heat capacity  $C_p$  ( $\text{J kg}^{-1} \text{K}^{-1}$ ); for grassland  $C_v$  was found in the range between 2000 and 20,000  $\text{J m}^{-2} \text{K}^{-1}$ . For the bulk conductance  $\lambda_m/\delta_m$ , values between 3 and 7  $\text{W m}^{-2} \text{K}^{-1}$  are reported (Duynkerke, 1991; Van de Wiel et al., 2003); see Table IV for an overview of proposed  $\lambda_m/\delta_m$  values. For the current study with an isolating conductance layer, we adopted  $C_v = 2090 \text{ J m}^{-2} \text{K}^{-1}$  and  $\lambda_m/\delta_m = 5 \text{ W m}^{-2} \text{K}^{-1}$ . Although the heat capacity of the isolating layer depends on various factors and is a rather uncertain variable, we adopt the range 2000–20,000  $\text{J m}^{-2} \text{K}^{-1}$  in our sensitivity analysis.

The introduction of a stagnant air layer (Figure 7) in the model leads also to strong surface cooling, resulting in a final temperature of 256.2 K

TABLE IV  
Overview of reported bulk heat conductance values.

Reference	Bulk heat conductance ( $\text{W m}^{-2} \text{K}^{-1}$ )
Van de Wiel et al. (2002a)	2.5
Duynkerke (1999)	3.0
Van Ulden and Holtslag (1985)	5
Steeneveld et al. (2004)	6.8
Viterbo and Beljaars (1995)	7

(Figure 8). The boundary layer has become less deep (170 m instead of 220 m with the heat diffusion equation), with a LLJ of  $9.1 \text{ m s}^{-1}$  at 125 m above the surface. The integrated cooling aggregates to  $IC = -736.3 \text{ K m}$ . Figure 9 shows the sensitivity of the final potential temperature and wind speed profiles to the bulk conductance coefficient  $\lambda_m/\delta_m$ . For the range of  $2 < \lambda_m/\delta_m < 20$ , the modelled surface temperature varies between 261.2 and 252.9 K. This large sensitivity is an important result, since a conductance layer is actually required in the model for a realistic behaviour of  $T_s$  in the case when vegetation is present (see Section 1).

The boundary-layer depth and stability also depend heavily on this bulk conductance parameter as well as the strength and altitude of the LLJ maximum. For full representation of the SBL in atmospheric models, an adequate estimate of this surface parameter is therefore of major importance. Note that this parameter is also a key parameter in modelling both intermittent turbulence and the oscillatory behaviour of the SBL temperature, as indicated by modelling results of van de Wiel et al. (2002a, 2003). Interestingly, the present multi-layer single column model revealed oscillations of a similar type (amplitude and period, not shown), as in the model results of ReVelle (1993) and in the simple bulk model results of van de Wiel et al. (2002a). It is tempting to investigate this subject in more detail, but it is beyond the scope of the present study.

Besides the processes represented by the surface energy budget and the turbulent mixing processes, radiation divergence has an important impact on the structure of the SBL (see Andre and Mahrt, 1982 and GB81). Both studies report a three-layer structure during the quasi-steady state of the SBL: a strong inversion near the surface, dominated by radiation divergence, a thick layer in the middle of the SBL dominated by turbulence, and an inversion layer dominated by radiative transport. For the current case study with moderate mechanical forcing using a geostrophic wind  $U_g = 8 \text{ m s}^{-1}$ , the impact of radiation divergence applying the model of GB81 (with a uniform specified specific humidity of  $0.1 \text{ g kg}^{-1}$ ) is small (not

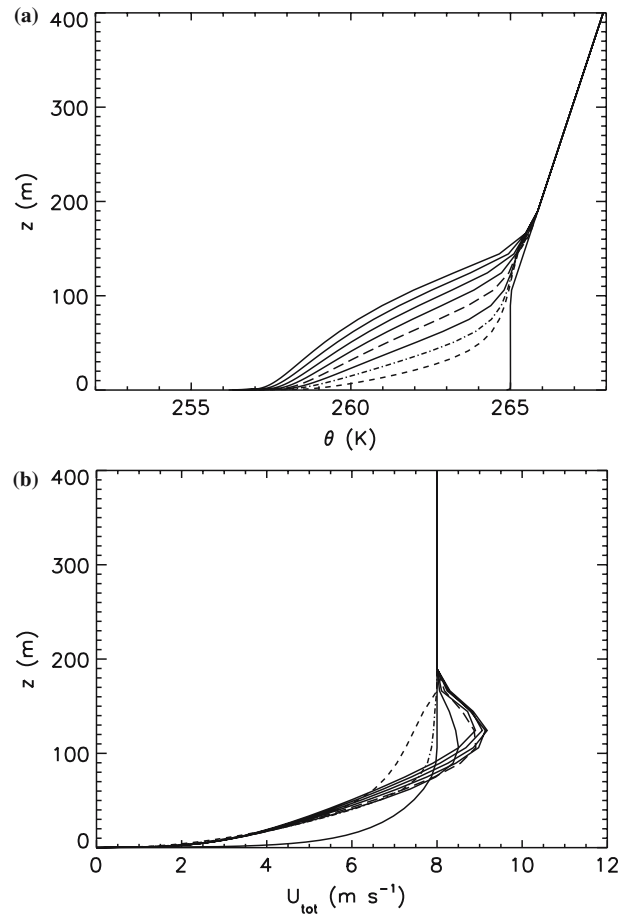


Figure 8. Potential temperature (a) and wind speed (b) development and structure in the alternative of solving the surface energy balance with a bulk conductance method and a stagnant air layer.

shown). With this strong mechanical forcing, the impact of radiation divergence is slightly noticeable near the surface: the inversion near the surface is smoother than in the reference case. In the ‘bulk’ of the boundary layer, hardly any impact is seen.

However, it is to be expected that for weaker mechanical forcing the relative impact of radiation will increase. Figure 10 shows the potential temperature development for  $U_g = 3 \text{ m s}^{-1}$ , with and without radiation calculations incorporated for the bulk conductance method (using  $C_v = 20,900 \text{ J m}^{-2} \text{ K}^{-1}$ ) and a vertical resolution of 2 m. The boundary layer is very thin in this case, but the structure is heavily dominated by radiation. In the latter case, the temperature inversion is more elevated and the vertical temperature gradients are weaker (radiative averages tend to smooth out large

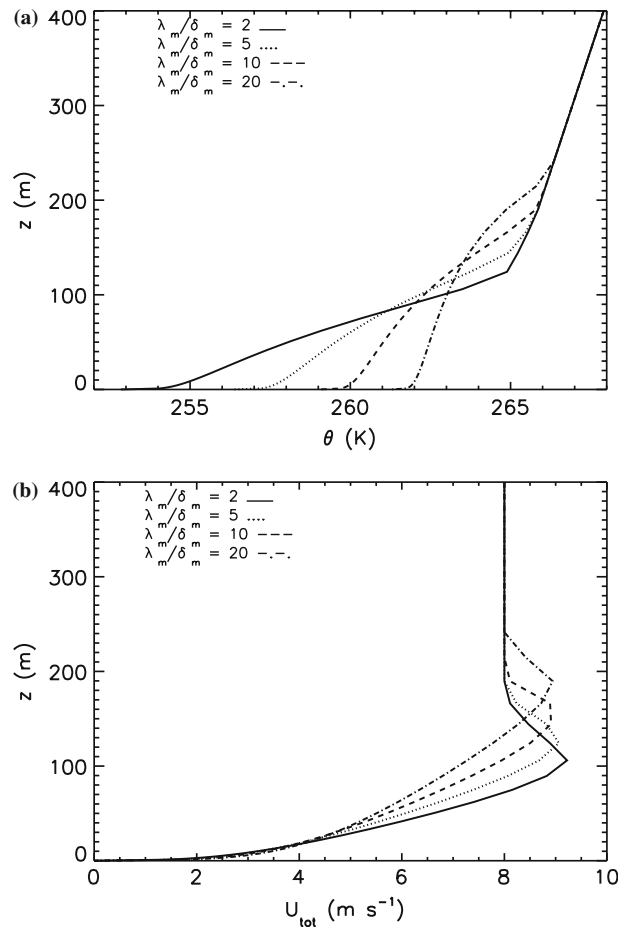


Figure 9. Sensitivity of the final profiles for potential temperature (a) and wind speed (b) to the bulk heat conductance ( $\lambda_m/\delta_m$ ).

temperature gradients). Thus during weak wind conditions radiation divergence is an important process in SBL development, and is required especially on nights when turbulence is nearly absent (e.g. the third night in Figure 1). This is in agreement with the work of Ha and Mahrt (2003) and earlier findings.

To examine the impact of vertical resolution in the radiation scheme, Figure 10c shows the cooling profiles due to radiation divergence for the last run, after 4 h of cooling. One result is based on the original grid mesh of 2 m and the other result is obtained by using a 20 m grid mesh, both using the same temperature and humidity profiles in the calculations. A clear distinction is seen: the coarser grid mesh results in an underestimate

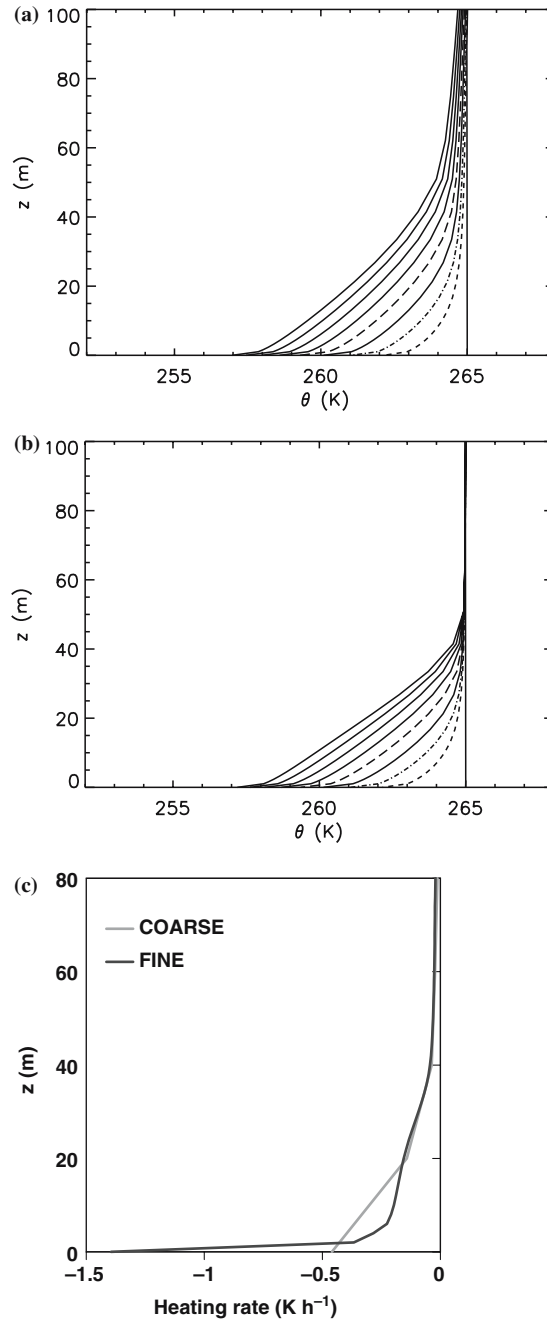


Figure 10. Potential temperature development with (a) and without (b) the radiation scheme for a geostrophic wind speed of  $3 \text{ m s}^{-1}$  and  $C_v = 20,900 \text{ J m}^{-2} \text{ K}^{-1}$ ; (c) radiative cooling for high (2 m) and low (20 m) vertical resolution after 4 hours' cooling.

of the cooling due to radiation divergence. This is in close agreement with the findings of Ha and Mahrt (2003).

## 5. Conclusions

Point of departure in the current paper is the reference GABLS single column model intercomparison study that uses a prescribed surface cooling rate as a boundary condition (Cuxart et al., 2006). Both theory and observations reported in the literature indicate that a simple extension of this reference case, by taking into account the surface energy budget, is necessary to attain a realistic boundary condition (since, in reality, the surface temperature  $T_s$  and surface sensible heat flux  $\overline{w'\theta'}_s$  are dynamically interdependent). In the present study, this extension is pioneered in two different ways:

- At first, we include the surface energy balance and solve the diffusion equation for heat in the ice. This coupling between the atmosphere and the land surface results in stronger surface cooling and a thinner boundary layer compared to the reference case. A clear dependence on the vertical grid spacing in the ice is found. Coarse resolution in the ice gives a stronger surface cooling, and a thinner boundary layer that is, on average, more stable. In contrast, a coarser resolution in the atmosphere has little effect on the results, as was also found by Delage (1997).
- In the second method we introduce a bulk conductance layer of stagnant air at the surface. This is a realistic extension representing cases when (low) vegetation or snow cover is present. Moreover, from previous studies (van de Wiel et al., 2002a) it is clear that such a coupling may lead to additional internal dynamics. In the present study, the implementation of a bulk conductance layer results in stronger surface cooling and a thinner boundary layer compared to the reference case. Also, the SBL development shows strong sensitivity to the numerical value of the bulk conductance of the stagnant air layer. So, the impact of this particular surface boundary condition is large, even in its most simple form.

Naturally, the bulk conductance depends on the land use, vegetation cover and snow/no snow cover as well, and its value is required as input in large-scale models (from some land-use classification). Additionally, the current study confirms that the impact of clear air radiation divergence (as compared to turbulence flux divergence) is mostly relevant at low geostrophic winds (consistent with the findings of Estournel and Guedalia, 1985, and others).

The present study on atmosphere-surface coupling (and similar studies on length scale formulations) show an evident impact on the structure and development of the SBL. These issues call for additional validation with detailed observations of surface fluxes, vertical temperature profiles, and the boundary-layer depth, e.g. as available for CASES-99 (Poulos et al., 2002), SABLES-98 (Cuxart et al., 2000), for Cabauw (Beljaars and Bosveld, 1997), or for more heterogeneous characteristics such as in Lindenberg, Germany (Beyrich et al., 2002). For modelling these real cases special attention should be paid to the interaction of the SBL with the surface and soil.

### Acknowledgements

The authors wish to thank Dr. Gunilla Svensson (Stockholm University) for her useful suggestions on an earlier version of the manuscript. Furthermore we acknowledge our colleague Dr. Arnold Moene and the participants in the GABLS LES model intercomparison, whose model output was used in this study.

### References

- Andre J. C. and Mahrt, L.: 1982, 'The Nocturnal Surface Inversion and Influence of Clear-air Radiative Cooling', *J. Atmos. Sci.* **39**, 864–878.
- Beare, R. J., MacVean, M. K., Holtslag, A. A. M., Cuxart, J., Golaz, J. C., Jimenez, M. A., Khairoutdinov, M., Kosovic, B., Lewellen, D., Lund, T. S., Lundquist, J. K., McCabe, A., Moene, A. F., Noh, Y., Raasch S., and Sullivan, P. P.: 2006, 'An Intercomparison of Large-eddy Simulations in the Stable Boundary-Layer', *Boundary-Layer Meteorol.*, in press.
- Beljaars, A. C. M. and Holtslag, A. A. M.: 1991, 'Flux Parameterization over Land Surfaces for Atmospheric Models', *J. Appl. Meteorol.* **30**, 327–341.
- Beljaars, A. C. M. and Bosveld, F. C.: 1997, 'Cabauw Data for Validation of Land Surface Parameterization Schemes', *J. Climate* **10**, 1172–1193.
- Beljaars, A. C. M. and Viterbo, P.: 1998, 'Role of the Boundary Layer in a Numerical Weather Prediction Model', in A. A. M. Holtslag and P. G. Duynkerke (eds.), *Clear and Cloudy Boundary Layers*, Royal Netherlands Academy of Arts and Sciences, Amsterdam, 372 pp.
- Best, M. J.: 1998, 'A Model to Predict Surface Temperatures', *Boundary-Layer Meteorol.* **88**, 279–306.
- Beyrich, F.: 1997, 'Mixing Height Estimation from Sodar Data- A Critical Discussion', *Atmos. Environ.* **31**, 3941–3953.
- Beyrich, F., De Bruin, H. A. R., Meijninger, W. M. L., Schipper J. W., and Lohse, H.: 2002, 'Results from One-Year Continuous Operation of a Large Aperture Scintillometer over a Heterogeneous Land Surface', *Boundary-Layer Meteorol.* **105**, 85–97.
- Brost, R. A. and Wyngaard, J. C.: 1978, 'A Model Study of the Stably Stratified Planetary Boundary Layer', *J. Atmos. Sci.* **35**, 1427–1440.

- Bruin, H. A. R. de: 1994, 'Analytic Solutions of the Equations Governing the Temperature Fluctuation Method', *Boundary-Layer Meteorol.* **68**, 427–432.
- Coulter, R. L. and Doran, J. C.: 2002, 'Spatial and Temporal Occurrences of Intermittent Turbulence during CASES-99', *Boundary-Layer Meteorol.* **105**, 329–349.
- Cuxart, J., Yagüe, C., Morales, G., Terradellas, E., Orbe, J., Calvo, J., Fernández, A., Soler, M. R., Infante, C., Buenestado, P., Espinalt, A., Joergensen, H. E., Rees, J. M., Vilà, J., Redondo, J. M., Cantalapiedra, I. R. and Conangla, L.: 2000, 'Stable Atmospheric Boundary-Layer Experiment in Spain (SABLES 98): A Report', *Boundary-Layer Meteorol.* **96**, 337–370.
- Cuxart, J., Holtslag, A. A. M., Beare, R. J., Bazile, E., Beljaars, A. C. M., Cheng, A., Conangla, L., Ek, M., Freedman, F., Hamdi, R., Kerstein, A., Kitagawa, H., Lenderink, G., Lewellen, D., Mailhot, J., Mauritsen, T., Perov, V., Schayes, G., Steeneveld, G. J., Svensson, G., Taylor, P. A., Weng, W., Wunsch, S., and Xu, K.-M.: 2006, 'A Single-Column Model Intercomparison for a Stably Stratified Atmospheric Boundary Layer', *Boundary-Layer Meteorol.*, in press.
- Delage, Y.: 1974, 'A Numerical Study of the Nocturnal Atmospheric Boundary-Layer', *Quart. J. Roy. Meteorol. Soc.* **100**, 351–364.
- Delage, Y.: 1997, 'Parameterising Sub-grid Scale Vertical Transport in Atmospheric Models Under Statically Stable Conditions', *Boundary-Layer Meteorol.* **82**, 23–48.
- Delage, Y., Barlett, P. A., and McCauchy, J. H.: 2002, 'Study of 'Soft' Night Time Surface Layer Decoupling over Forest Canopies in a Land-Surface Model', *Boundary-Layer Meteorol.* **103**, 253–276.
- Derbyshire, S. H.: 1999, 'Boundary-layer Decoupling over Cold Surfaces as a Physical Boundary Instability', *Boundary-Layer Meteorol.* **90**, 297–325.
- Duynkerke, P. G.: 1991, 'Radiation Fog: A Comparison of Model Simulation with Detailed Observations', *Mon. Wea. Rev.* **119**, 324–341.
- Duynkerke, P. G.: 1999, 'Turbulence, Radiation and Fog in Dutch Stable Boundary-Layers', *Boundary-Layer Meteorol.* **90**, 447–477.
- Estournel, C. and Guedalia, D.: 1985, 'Influence of Geostrophic Wind on Atmospheric Nocturnal Cooling', *J. Atmos. Sci.* **42**, 2695–2698.
- Galmarini, S., Beets, C., Duynkerke, P. G., and Vila-Guerau de Arellano, J.: 1998, 'Stable Nocturnal Boundary-layers: a Comparison of One-dimensional and Large-eddy Simulation Models', *Boundary-Layer Meteorol.* **88**, 181–210.
- Garratt, J. R. and Brost, R. A.: 1981, 'Radiative Cooling Effects within and above the Nocturnal Boundary-Layer', *J. Atmos. Sci.* **38**, 2730–2746.
- Ha, K. J. and Mahrt, L.: 2003, 'Radiative and Turbulent Fluxes in the Nocturnal Boundary-Layer', *Tellus* **55A**, 317–327.
- Holtslag, A. A. M. and Bruin, H. A. R. de: 1988, 'Applied Modelling of the Nighttime Surface Energy Balance over Land', *J. Appl. Meteorol.* **27**, 689–704.
- Holtslag, A. A. M.: 1998, Modeling of Atmospheric Boundary Layers, in A. A. M. Holtslag and P. G. Duynkerke (eds.), *Clear and Cloudy Boundary Layers*, Royal Netherlands Academy of Arts and Sciences, Amsterdam, 372 pp.
- Holtslag, A. A. M., Beare R. J., and Cuxart Rodamillans, J.: 2003, 'GABLS Workshop on Stable Boundary Layers', *GEWEX News*, *GEWEX newsletter* **13**(4), 11–13.
- Hunt, J. C. R., Kaimal, J. C., and Gaynor, J. E.: 1985, 'Some Observations of Turbulence Structure in Stable Layers', *Quart. J. Roy. Meteorol. Soc.* **111**, 793–815.
- Koivusalo, H., Heikinheimo, M., and Karvonen, T.: 2001, 'Test of a Simple Two-layer Parameterisation to Simulate the Energy Balance and Temperature of a Snow Pack', *Theor. Appl. Climatol.* **70**, 65–79.

- Kosovic, B. and Curry, J. A.: 2000, 'A Large Eddy Simulation study of a Quasi-Steady, Stably Stratified Atmospheric Boundary-Layer', *J. Atmos. Sci.* **57**, 1052–1068.
- Louis, J. F.: 1979, 'A Parametric Model of Vertical Eddy Fluxes in the Atmosphere', *Boundary-Layer Meteorol.* **17**, 187–202.
- Mahrt, L.: 1987, 'Grid-averaged Surface Fluxes', *Mon. Wea. Rev.* **115**, 1550–1560.
- Mahrt, L. and Vickers, D.: 2002, 'Contrasting Vertical Structures of Nocturnal Boundary layers', *Boundary-Layer Meteorol.* **105**, 351–363.
- Nieuwstadt, F. T. M. and Driedonks, A. G. M.: 1979, 'The Nocturnal Boundary-Layer: A Case Study Compared with Model Calculations', *J. Appl. Meteorol.* **18**, 1397–1405.
- Nieuwstadt, F. T. M.: 1984, 'The Turbulent Structure of the Stable, Nocturnal Boundary-layer', *J. Atmos. Sci.* **41**, 2202–2216.
- Oke, T. R.: 1978, *Boundary-Layer Climates*. Methuen and Co., London, United Kingdom, 372 pp.
- Rama Krishna, T. V. B. P. S., Sharan, M., and Aditi: 2003, 'Mean Structure of the Nocturnal Boundary-Layer under Strong and Weak Wind Conditions: EPRI Case Study', *J. Appl. Meteorol.* **42**, 952–969.
- ReVelle, D. O.: 1993, 'Chaos and "Bursting" in the Planetary Boundary-Layer', *J. Appl. Meteorol.* **32**, 1169–1180.
- Steenefeld, G. J., Wiel, B. J. H. van de and Holtslag, A. A. M.: 2004, 'Modelling the Evolution of the Nocturnal Boundary-Layer for Three Different Nights in CASES-99', *16th Symposium on Boundary-Layer and Turbulence*, Portland, Maine, U.S.A., 9–13 Aug. 2004, Amer. Meteorol. Soc., Boston, p. 4.3.
- Stull, R. B.: 1988, *An Introduction to Boundary-Layer Meteorology*, Kluwer Academic Publishers, Dordrecht, 666 pp.
- Viterbo, P. and Beljaars, A. C. M.: 1995, 'An Improved Land Surface Parameterization in the ECMWF Model and its Validation', *J. Climate* **8**, 2716–2748.
- Viterbo, P., Beljaars, A., Mahfouf, J.F., and Teixeira, J.: 1999, 'The Representation of Soil Moisture Freezing and its Impact on the Stable Boundary-Layer', *Quart. J. Roy. Meteorol. Soc.* **125**, 2401–2426.
- Wiel, B. J. H. van de, Ronda, R. J., Moene, A. F., Bruin, H. A. R. de and Holtslag, A. A. M.: 2002a, 'Intermittent Turbulence and Oscillations in the Stable Boundary-Layer over Land. Part I: A Bulk Model', *J. Atmos. Sci.* **59**, 942–958.
- Wiel, B. J. H. van de, Moene, A. F., Ronda, R. J., Bruin, H. A. R. de and Holtslag, A. A. M.: 2002b, 'Intermittent Turbulence and Oscillations in the Stable Boundary-Layer over Land. Part II: A System Dynamics Approach', *J. Atmos. Sci.* **59**, 2567–2581.
- Wiel, B. J. H. van de, Moene, A. F., Hartogensis, O. K., Bruin, H. A. R. de and Holtslag, A. A. M.: 2003, 'Intermittent Turbulence and Oscillations in the Stable Boundary-Layer over Land. Part III: a Classification for Observations during CASES-99', *J. Atmos. Sci.* **60**, 2509–2522.
- Wiel, B. J. H. van de, Moene, A. F., and Steeneveld, G. J.: 2004, 'Stable Boundary Layer Decoupling: Towards a Linear Stability Analysis', *16th Symposium on Boundary-Layer and Turbulence*, Portland, Maine, U.S.A., 9–13 Aug. 2004, Amer. Meteorol. Soc., Boston, p. 4.18.